FINITE ELEMENT ANALYSIS OF HONEYCOMB MEMBRANE-TYPE ACOUSTIC METAMATERIAL

Zacharie Laly [*1, 2], Christopher Mechefske [†2], Sebastian Ghinet [‡3], Behnam Ashrafi [♦4], and Charly T. Kone [♯3]

[1]CRASH, Centre de Recherche Acoustique-Signal-Humain, Université de Sherbrooke, Québec, Canada.
[2]Department of Mechanical and Materials Engineering, Queen's University, Kingston, Ontario, Canada.
[3]Aerospace, National Research Council Canada, Ottawa, Ontario, Canada.
[4]Aerospace Manufacturing Technology Center, National Research Council Canada, Montreal, Québec, Canada.

Résumé

Dans cet article, un métamatériau acoustique constitué d'une structure en nid d'abeille avec des couches de membrane intégrées est étudié à l'aide de la méthode des éléments finis. Ce matériau léger présente une excellente perte par transmission en basse fréquence. La structure en nid d'abeille avec deux et trois couches de membranes intégrées est analysée numériquement et les effets du nombre de couches de membranes et de l'épaisseur du gap d'air entre les membranes sont illustrés. Les influences des propriétés de matériau et de l'épaisseur de la membrane sur la perte par transmission et l'amplitude et la forme du mode du déplacement à différentes fréquences sont présentées. Il est montré que la perte par transmission augmente sur une large bande fréquentielle lorsque la taille des cellules du nid d'abeille diminue tandis que l'amplitude du déplacement de la membrane est réduite et la forme du mode du déplacement est affectée. Il est observé que la perte par transmission présente de multiples pics de résonance au fur et à mesure que l'épaisseur de la membrane est réduite. Une amélioration de la perte par transmission est observée autour des fréquences anti-résonnantes en augmentant le facteur d'amortissement de la membrane, ce qui provoque une réduction des pics de résonance du déplacement et de la perte par transmission. Le métamatériau étudié peut être utile dans de nombreuses applications d'ingénierie de contrôle du bruit.

Mots clefs : Métamatériau acoustique, structure en nid d'abeille, membrane, perte par transmission, matériau léger.

Abstract

In this paper, a honeycomb membrane-type acoustic metamaterial made of a honeycomb structure with embedded membrane layers is investigated using the finite element method. This lightweight material presents excellent transmission loss (TL) at low frequency. Honeycomb structures with two and three embedded membrane layers are analyzed numerically and the effects of the number of membrane layers and of the thickness of the air gap between membranes are illustrated. Also, the influences of the membrane material properties and thickness on the TL and displacement magnitude and mode shape at different frequencies are presented. It is shown that the TL increases over a large frequency band when the honeycomb cell size decreases while the displacement magnitude of the membrane is reduced and the mode shape is affected. It is observed that the TL presents multiple resonant peaks as the thickness of the membranes is reduced. An improvement of the TL is observed around the anti-resonant frequencies by increasing the damping loss factor of the membrane, which causes a reduction of the resonant displacement magnitude and TL peaks amplitude. The investigated metamaterial can be useful in many noise control engineering applications.

Keywords: Acoustic metamaterial, honeycomb structure, membrane, transmission loss, lightweight material.

1 Introduction

Lightweight materials are often desirable and used in many applications such as in the aerospace and automotive industries. One critical shortcoming of these lightweight materials is their poor sound transmission loss (TL) because of the mass law, which states that the noise transmission trough a material is inversely proportional to the surface mass of the panel and the frequency. This requires a large thickness of lightweight materials to achieve low-frequency acoustic attenuation. An optimal design of lightweight material with a high TL would therefore be interesting. Li et al. [1] investigated experimentally the TL of a lightweight multilayer honeycomb membrane-type acoustic metamaterial (MAM). They illustrated a significant sound insulation performance of the proposed structures by comparison with the traditional honeycomb structure with minimal mass increase. Sui et al. [2] and Lu et al. [3] studied a honeycomb acoustic metamaterial made of a lightweight flexible rubber material layer sandwiched between two layers of honeycomb cell plates. The structure presented negative mass density at frequencies below the first natural frequency, which results in excellent TL with minimum weight-penalty. Nguyen et al. [4] presented a double-

[*] zacharie.laly@usherbrooke.ca
[†] chris.mechefske@queensu.ca
[‡] sebastian.ghinet@nrc-cnrc.gc.ca
[♦] behnam.ashrafi@nrc-cnrc.gc.ca
[♯] tenoncharly.kone@nrc-cnrc.gc.ca

layer membrane-type acoustic metamaterial (DMAM) using theoretical and numerical analysis. They performed experimental tests on an acoustic panel made of an 8 x 8 DMAM array and showed that the transmission loss ranges from 40 dB to 59 dB in the frequency band 0.45–1.48 kHz, breaking the mass density law. Yang et al. [5] investigated lightweight membrane-type metamaterials made of a circular elastic membrane with a small weight attached at the center with fixed outer boundary. A negative effective mass was obtained at low frequency and the sound insulation was far higher than the one predicted by the mass law. Li et al. [6] proposed a theoretical method to predict the transmission loss of acoustic micro-membranes and showed significant enhancement of the sound insulation at low frequency. The influences on the TL of the membrane geometrical parameters such as the thickness and the surface area are illustrated in their study. Qiu et al. [7] proposed a theoretical method to study an array of membranes mounted in a lattice-like frame. They investigated the influence of the frame vibration and showed how the frames affect the vibration and transmission loss characteristics of the membranes. They derived an analytical expression of the TL by coupling the vibration of the frame and the membranes where the frame and membranes are considered in parallel. It was observed that the global response of the assembly is no longer dominated by the membranes but by the frame as the assembly becomes larger. Finite element method was used by Laly et al. [8] to model a honeycomb structure with embedded membrane layers. An improvement of the transmission loss at low frequency was illustrated. Gao et al. [9] investigated numerically and experimentally the low frequency sound insulation performance of a deformable honeycomb acoustic metamaterial made of honeycomb structures with embedded ethylene-vinyl acetate (EVA) rubber material. They observed that the investigated metamaterial has a better sound insulation than traditional sound insulation structures and its transmission loss can be adjusted by the dislocation, compression, and tensile deformation. Hu et al. [10] studied a type of membrane-sandwich plate metamaterial constituted by sandwich panels with embedded membranes with attached masses. They presented the sound insulation properties for different masses and illustrated the influence of the mass size on the TL. Their experimental analysis showed excellent low frequency sound insulation performance. Ma et al. [11] reported numerical and experimental analysis on a type of 2D multiple cells lumped ultrathin lightweight plate-type acoustic metamaterials structures, which illustrates good TL in the low frequency range. The basic unit cell of the metamaterials was made of an ultrathin stiff nylon plate clamped by two elastic ethylene-vinyl acetate copolymer. Marinova et al. [12] modelled a low frequency noise shield made of a double wall system, which includes two membrane-type acoustic metamaterials panels in the enclosed cavity. The MAM panel comprises a thin elastic mass-loaded membrane and a supporting frame. They validated the numerical simulations with experimental measurements. Zhou et al. [13] presented a method to broaden the low frequency bandwidth of sound insulation by designing a flexible membrane-type acoustic metamaterial sample that is made of a homogenous membrane and a perforated EVA copolymer plate. They created holes of different diameters in the flexible EVA plate and showed that the lower limit, the peak frequency and the upper limit of the TL bandwidth can be regulated by the lumped coupling resonance, anti-resonance and local resonance modes of the relevant areas. They proposed two MAM samples and the results of the TL illustrated improved bandwidths. Mo et al. [14] investigated a structure of acoustic micro membrane metamaterial where each micro membrane is a small square held within a larger lattice frame. Using theoretical and numerical simulations that include the vibration of the frame, they showed how the global TL of the assembly is related to the geometrical parameters of the micro membrane cells and the lattice. They noted that the frame should be strong enough to provide rigid boundaries to the micro membranes in order to improve the TL. Langfeldt et al. [15] presented an analytical method to predict the TL of baffled panels with multiple subwavelength sized membrane-type acoustic metamaterial unit cells using effective surface mass density concept. They studied the influence of flexible MAM unit cell edges and observed that the compliance of the edges has small impact on the TL except in the stiffness-controlled regime.

The development of lightweight materials with good transmission loss at low frequency is a challenge.

The work presented here uses the finite element method to investigate a honeycomb membrane type acoustic metamaterial constituted by a honeycomb structure with embedded membrane layers. This analysis considers a lightweight material design with a high sound attenuation efficiency. The transmission loss of the metamaterial is significantly improved especially at low frequency while the TL of the honeycomb core structure alone is zero over the entire frequency range. The influence of the membrane material properties on the TL is analyzed. By reducing the thickness of the membrane, the displacement magnitude of the membrane and the TL show multiple resonant peaks. The impacts of the honeycomb cell size on the TL and the membrane displacement magnitude and mode shape are studied numerically as well as the effect of the membrane damping loss factor. The honeycomb with two and three integrated membrane layers is studied numerically and the influences of the number of membrane layers as well as the impact of the air gap between the membranes are demonstrated. The numerical analysis is described in section 2. In section 3, the results of different parametric analysis are shown and finally section 4 presents the numerical investigations on honeycomb structure with multiple embedded membrane layers.

2 Honeycomb structure with embedded membrane design

Honeycomb structures used in many applications are lightweight and offer good stiffness. In general, lightweight structures are not efficient in acoustic attenuation especially at low frequencies and this is due to the mass law. The integration of a membrane within honeycomb structures can present both the characteristic of lightness and good acoustic attenuation. In this paper, numerical analysis is performed on honeycomb structures with embedded membranes for transmission loss improvement. This is a honeycomb membrane-type acoustic

metamaterial where the impacts of the honeycomb cell size and the membrane properties on the transmission loss are analyzed using finite element method. In Fig. 1, a honeycomb structure with one embedded membrane layer is illustrated. The numerical simulations are conducted using acoustic-solid interaction of COMSOL Multiphysics to illustrate the contribution of the membrane in the transmission loss improvement. The membrane and the two honeycomb structures in Fig. 1 have the same lateral dimensions of 84 mm x 75 mm. An incident fluid and a transmission fluid are connected to the structure and all the air domains within the honeycomb cells are identified. The boundary between the membrane surface and each honeycomb structure layer is considered fixed in the numerical simulations. The geometry is shown in Fig. 1(a) and the mesh is presented in Fig. 1(b) which is a physics-controlled mesh with 144590 domain elements and 39707 boundary elements where the total degrees of freedom is 261100.

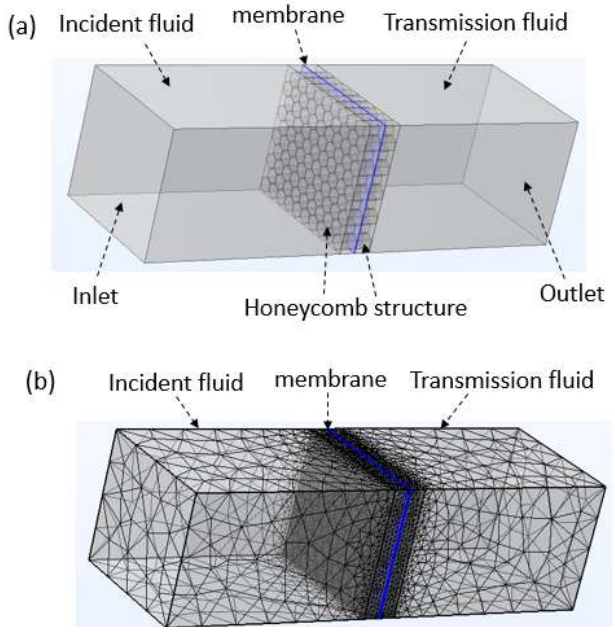

Figure 1: Numerical design of honeycomb structure with embedded membrane: (a) geometry (b) mesh.

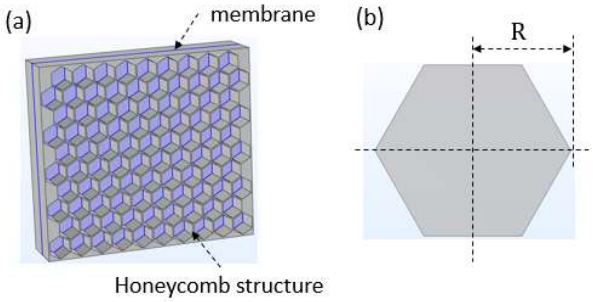

Figure 2: Honeycomb structure with embedded membrane: (a) honeycomb structure geometry (b) one honeycomb cell geometry.

Figure 2(a) shows the membrane that is sandwiched between two honeycomb structure layers and the geometry of one honeycomb cell is presented in Fig. 2(b). The dimension of the cell size is denoted by R and the thickness of each honeycomb structure layer is set to 10 mm.

The membrane is modeled as a linear isotropic elastic material using the solid mechanics module of COMSOL Multiphysics [8, 16, 17]. At the inlet and outlet planes as shown in Fig. 1, the plane wave radiation condition is applied to minimize the reflection of the acoustic waves. The material properties of the honeycomb structure namely the Young's modulus, the density, and the Poisson's ratio are 2.7 GPa, 1100 kg/m^3 and 0.38 respectively. The incident fluid and transmission fluid have the same length of 130 mm. A normal incidence plane wave with pressure amplitude of 1 Pa is applied on the inlet plane and the transmission loss is calculated numerically by the following relation [16-19]

$$TL = 10 \log_{10}\left(\frac{W_{in}}{W_{out}}\right), \tag{1}$$

where W_{in} and W_{out} are respectively the incoming power at the inlet plane and the outgoing power at the outlet plane given by

$$W_{in} = \int_{\partial\Omega} \frac{|p_0|^2}{2\rho c}, \qquad W_{out} = \int_{\partial\Omega} \frac{|p|^2}{2\rho c} \tag{2}$$

where c is the speed of sound in air, ρ is the density of air, and p_0 and p are the pressures at the inlet and outlet planes, respectively.

3 Finite element analysis results of honeycomb structures with embedded membrane

3.1 Numerical analysis of the effects of the membrane material properties

The geometry and mesh presented in Fig. 1 are used for the numerical analysis to evaluate the influence of the membrane material properties on the transmission loss. The honeycomb cell size R is set to 4.5 mm and the thickness of the membrane is 1 mm with a damping loss factor of zero. Different membrane material properties with Young's modulus that are gradually increased from 1.2 MPa to 100 MPa are considered. Table 1 summarizes the material properties of each membrane. Membrane 1 is a butyl rubber while membrane 3 is a silicone elastomer and membranes 2 and 4 are ethylene-vinyl acetate rubbers. Membrane 5 is a rubber material.

Table 1: Material properties of the membrane.

Membranes	Young's modulus (MPa)	Density (kg/m^3)	Poisson's ratio
1	1.2	910	0.4
2	5	660	0.45
3	12	1400	0.48
4	25	850	0.46
5	100	1100	0.49

The boundary between each membrane and each honeycomb structure layer is fixed. The transmission loss obtained using Eq. (1) for each membrane material in Table 1 is shown in Fig. 3. For the TL without a membrane within the honey-

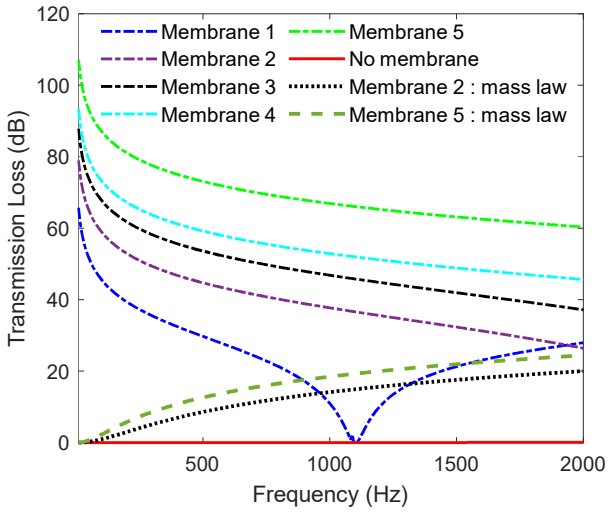

Figure 3: Effect of the membrane material properties on the transmission loss.

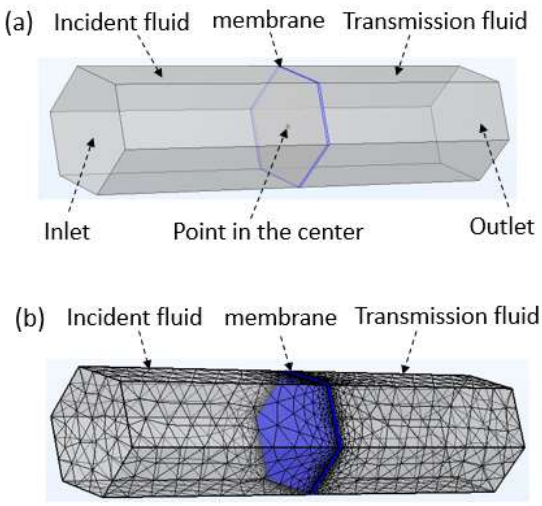

Figure 4: Honeycomb cell used for numerical analysis: (a) geometry (b) mesh.

comb structures (Fig. 3), the cell size is 4.5 mm and the thickness of the honeycomb is set to 20 mm. The TL predicted by the mass law is illustrated for membrane 2 and 5.

For the honeycomb structure alone without membrane, the transmission loss in Fig. 3 is zero over the entire frequency range. It does not attenuate any noise even though its stiffness and lightness can be interesting. The transmission loss with membrane 1 in Fig. 3 shows a drop at the frequency f=1110 Hz where the TL value is zero and below 500 Hz the TL is greater than 30 dB. With membrane 2, the TL is greater than 35 dB for frequencies lower than 1000 Hz while with membrane 5, the TL is over 65 dB for f<1000 Hz. When one considers a membrane with an increased Young's modulus, the TL increases over the entire frequency range. From membranes 2 to 5, the TL in Fig. 3 presents a large frequency band and is higher than the TL obtained by the mass law.

3.2 Effect of the membrane thickness

The influence of the membrane thickness *t* is investigated in the following where the numerical analysis was conducted using one honeycomb cell as illustrated in Fig. 4 with membrane fixed boundary conditions. The membrane is connected to an incident and transmission fluid. A plane wave radiation condition is applied on the inlet and outlet plans and a pressure of 1 Pa is applied on the inlet plane and the transmission loss is calculated using Eq. (1). The lateral boundary of the incident and transmission fluid are considered rigid and the point in the center of the membrane on the incident fluid side is located to extract numerically its displacement magnitude. The membrane is modeled using a solid mechanics module while the incident and transmission fluid domains are modeled with a pressure acoustics module of COMSOL and the boundaries between these two physics are the two membrane surfaces.

The membrane 2 of Table 1 is used and the honeycomb cell size R is set to 6 mm. The length of the incident and transmission fluid are both equal to 24 mm. The impact of the membrane thickness on its displacement mode shapes is presented in Figs. 5 and 6 for some frequencies. In Fig. 5, the

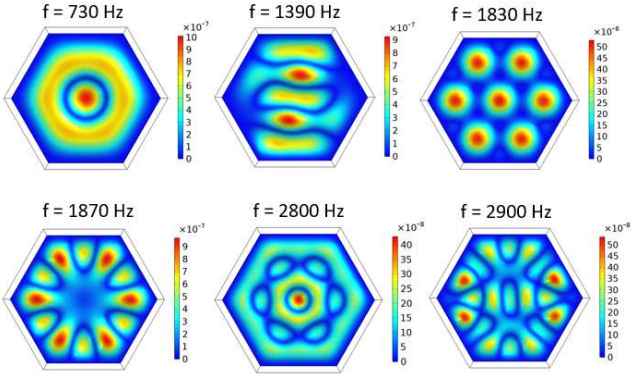

Figure 5: Displacement mode shapes of the membrane 2 for a thickness of 0.1 mm.

thickness of the membrane is set to 0.1 mm while in Fig. 6, the thickness is 0.25 mm. The displacement magnitude of the point in the center of the membrane (Fig. 4(a)) for different membrane thicknesses is illustrated in Fig. 7.

For each frequency, the membrane displacement mode shape changes in Figs. 5-6 when the thickness changes. With a thickness of 0.1 mm, one observes that the mode shapes in Fig. 5 are more complex than those in Fig. 6. The displacement magnitude of the point in the center of the membrane presented in Fig. 7 shows two peaks for a thickness of 0.1 mm at 555 Hz and 1880 Hz where the peak values are respectively 13.4 µm and 11.4 µm. For a thickness of 0.25 mm, the displacement values are 1.55 µm and 0.18 µm at 555 Hz and 1880 Hz respectively. With a thickness of 1 mm, the displacement tends towards zero. Thus, when the thickness of the membrane increases, the displacement magnitude decreases.

The impact of the membrane thickness on the transmission loss is shown in Fig. 8.

For a thickness of 1 mm, the transmission loss in Fig. 8 is greater than 25 dB with a wide attenuation band for frequencies below 1000 Hz and decreases when the thickness decreases. For t = 0.5 mm, the TL presents a drop around

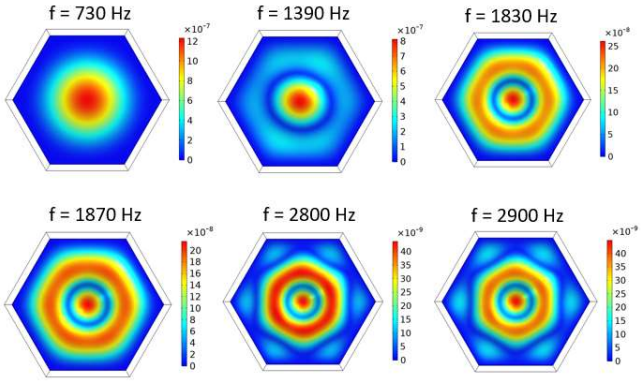

Figure 6: Displacement mode shapes of the membrane 2 for a thickness of 0.25 mm.

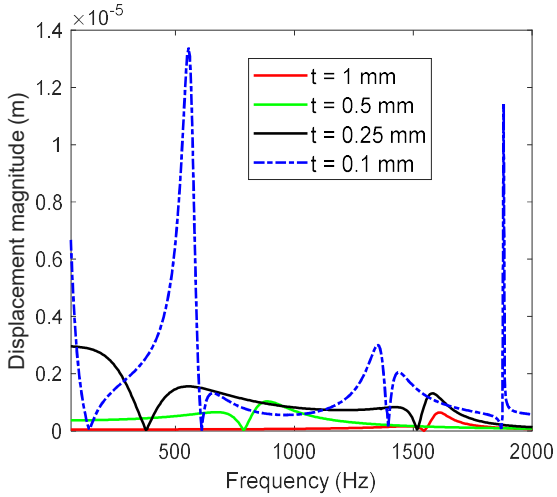

Figure 7: Effect of the membrane thickness on the displacement magnitude.

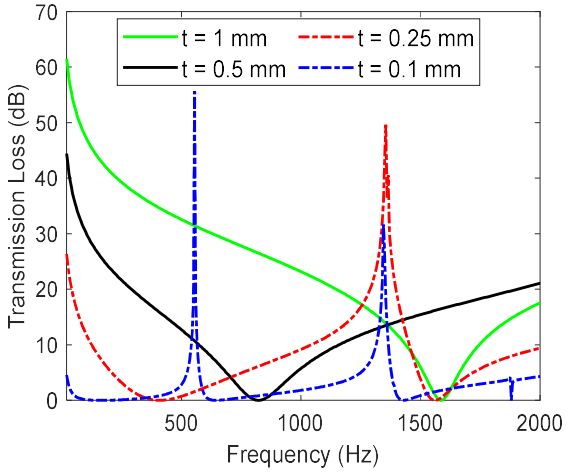

Figure 8: Effect of the membrane thickness on the transmission loss.

825 Hz where its value is zero. With a thickness of 0.25 mm, one observes a resonance peak at 1355 Hz where the TL value is 49 dB. Two TL resonance peaks are observed for a thickness of 0.1 mm at 555 Hz and 1345 Hz where the TL values are 55 dB and 32 dB respectively. Apart from these two resonant frequencies, the TL for t=0.1 mm is low and close to zero for f<450 Hz. Thus, when the thickness of the membrane increases, the TL is improved at low frequency with an increased attenuation frequency band.

3.3 Finite element analysis of the influence of the honeycomb cell size

The effect of the honeycomb cell size is analyzed numerically in this section using the geometry that is illustrated in Fig. 4. Membrane 2 of Table 1 with a thickness of 0.5 mm is considered with fixed boundary conditions and the cell size R is varied. The incident and transmission fluid have the same length, which is equal to 4R. Figure 9 shows the transmission loss for different honeycomb cell sizes. In Fig. 10, the displacement magnitude of the point in the center of the membrane (Fig. 4) is illustrated.

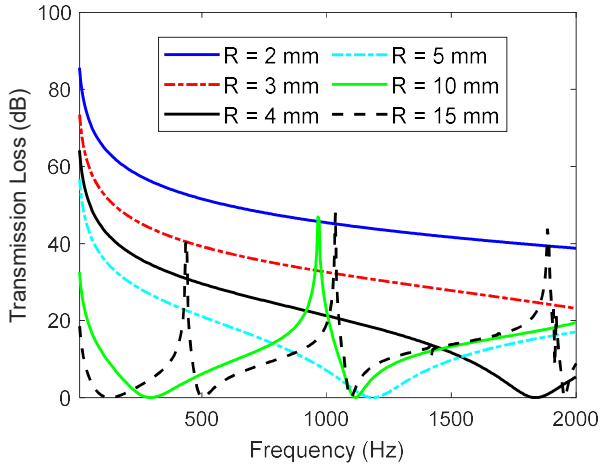

Figure 9: Effect of the cell size on the transmission loss for the membrane thickness of 0.5 mm.

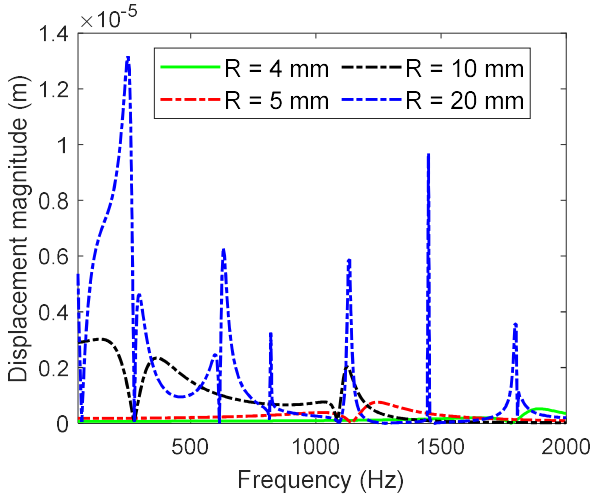

Figure 10: Effect of the cell size on the displacement magnitude for the membrane thickness of 0.5 mm.

The transmission loss in Fig. 9 is greater than 38 dB over the entire frequency range for R=2 mm and for R=3 mm, it is greater than 23 dB and increases when the frequency decreases. The TL drop for R=4 mm and R=5 mm is observed

around 1845 Hz and 1190 Hz respectively and for R=10 mm, the TL presents a resonant peak at 970 Hz with value of 46 dB. With a cell dimension of 15 mm, the TL exhibits 3 resonance peaks at 435 Hz, 1035 Hz and 1885 Hz where the TL values are 40 dB, 48 dB and 44 dB respectively. As the honeycomb cell size is reduced, the TL increases over the entire frequency range. The displacement magnitude in Fig. 10 of the point at the center of the membrane presents several resonance peaks for R=20 mm. When the honeycomb cell size decreases, the resonant peaks disappear and the amplitude of the displacement tends towards zero. The reduction of the honeycomb cell size leads to a reduction in the displacement amplitude, but the TL increases over the entire frequency band.

The influence of the honeycomb cell size on the displacement mode shapes of the membrane is illustrated in Figs. 11-13. These show the displacement mode shapes for honeycomb cell size R of 10 mm 15 mm and 20 mm respectively. The thickness of the membrane is set to 0.25 mm with fixed boundary conditions.

As the dimension of the honeycomb cell increases, the displacement mode shapes in Figs. 11-13 change at each frequency while the displacement amplitude presents more peaks in Fig. 10 as well as the TL in Fig. 9.

3.4 Analysis of the membrane damping loss factor

The impact of the membrane damping loss factor on the displacement and transmission loss were also investigated. One honeycomb cell as shown in Fig. 4 is considered with size R of 8 mm. The membrane 4 of Table 1 is used with a thickness of 1 mm and its boundary conditions are fixed. The isotropic loss factor η of the membrane is varied from zero to 40% and the transmission loss is presented in Fig. 14. Figure 15 shows the average surface displacement magnitude of the membrane for different loss factors.

In Fig. 14, one observes a drop in the TL for η=0 at 1850 Hz where the TL value is zero and the displacement at this frequency in Fig. 15 presents a peak with a value of 0.21 µm. When the loss factor η increases, the transmission loss around 1850 Hz increases and the peak of the displacement magnitude in Fig. 15 decreases. For η=0.1, the TL value at 1850 Hz is 10.56 dB in Fig. 14 and the displacement amplitude value is 0.063 µm. For η =0.4, the TL value at 1850 Hz is 20 dB while the peak of the displacement is 0.02 µm. Between 1655 Hz and 2060 Hz, the TL is improved when the loss factor η increases while the peak of the displacement magnitude is reduced.

One considers now the membrane 2 of Table 1 with fixed boundary conditions and the dimension of the honeycomb cell size R is set to 8 mm. In Figs. 16-17, the transmission loss is presented for different damping loss factors. In Fig. 16, the membrane thickness is set to 1 mm while in Fig. 17, the thickness is 0.25 mm.

The influence of the damping loss factor on the displacement magnitude and displacement mode shape at different frequencies is illustrated in Figs. 18-20 for a membrane thickness of 0.25 mm.

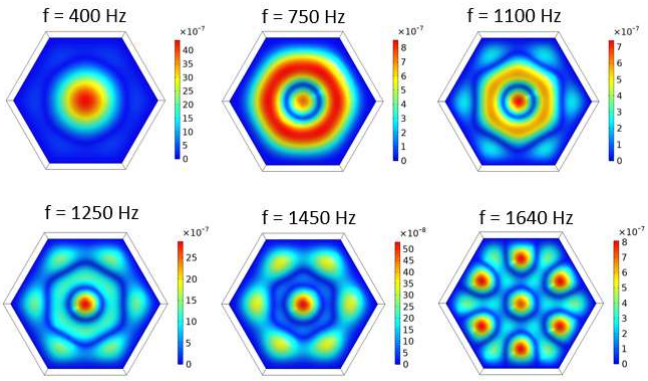

Figure 11: Displacement mode shape of the membrane for a cell size of 10 mm.

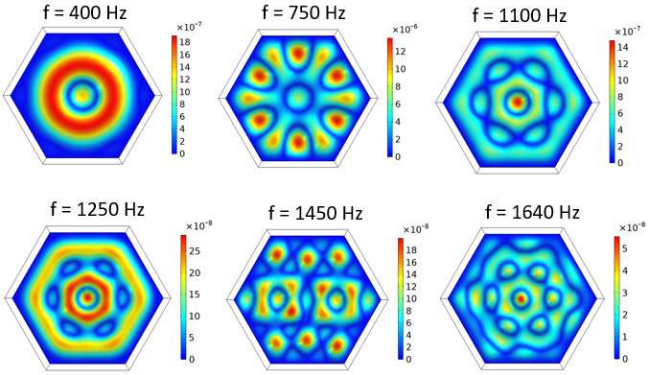

Figure 12: Displacement mode shape of the membrane for a cell size of 15 mm.

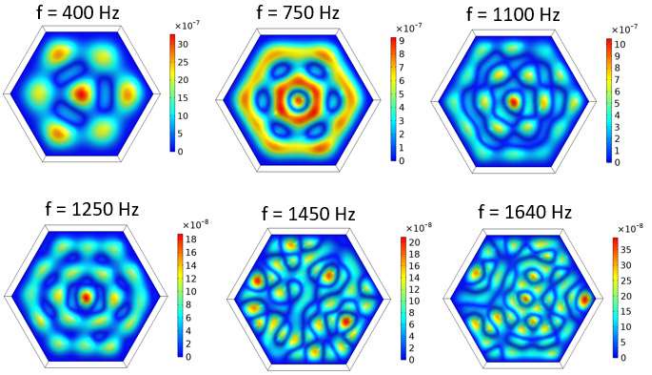

Figure 13: Displacement mode shape of the membrane for a cell size of 20 mm.

The displacement magnitude peaks in Fig. 18 decrease as the damping factor increases. In Fig. 16, the TL is improved around the anti-resonance frequencies of 930 Hz and 3225 Hz when the damping loss factor increases, on the other hand the resonance TL peak at 2760 Hz decreases. In Fig. 17, one observes also that the resonance TL peaks are reduced when the damping loss factor increases and the displacement modes in Figs. 19-20 are influenced.

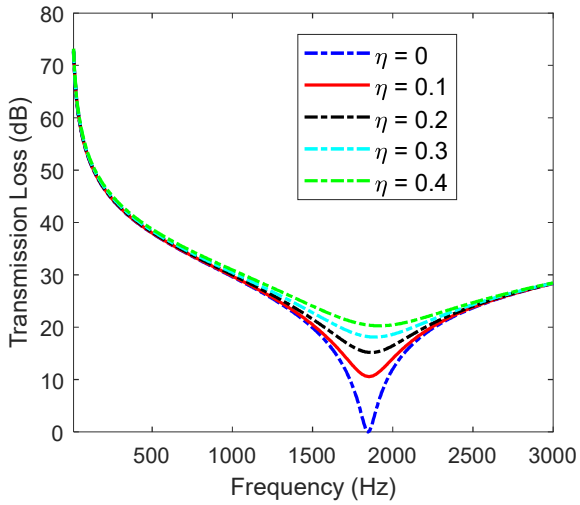

Figure 14: Effect of the membrane damping loss factor on the transmission loss.

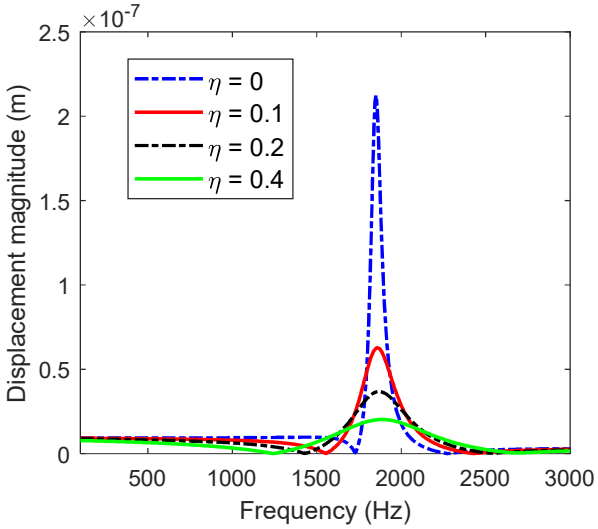

Figure 15: Effect of the membrane damping loss factor on the displacement magnitude.

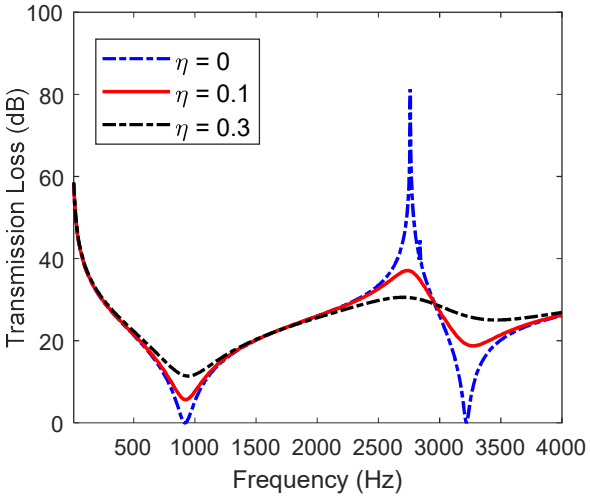

Figure 16: Effect of the membrane damping loss factor on the transmission loss for a membrane thickness of 1 mm.

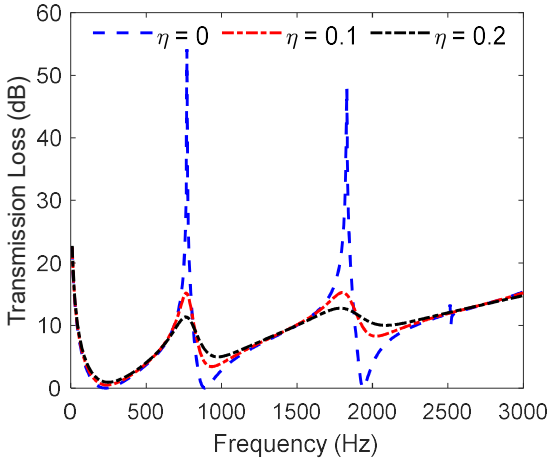

Figure 17: Effect of the membrane damping loss factor on the transmission loss for a membrane thickness of 0.25 mm.

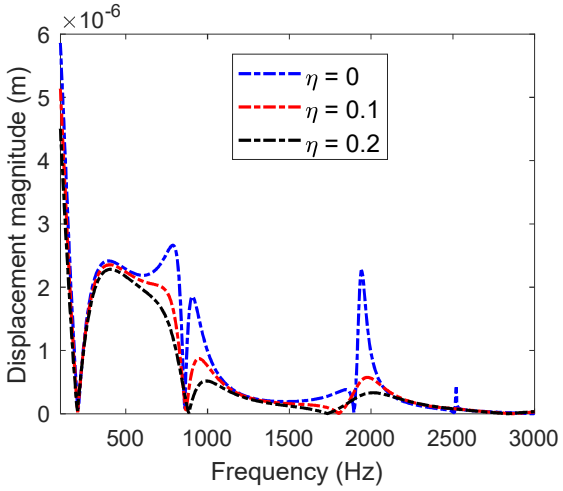

Figure 18: Effect of the membrane damping loss factor on displacement magnitude for a membrane thickness of 0.25 mm.

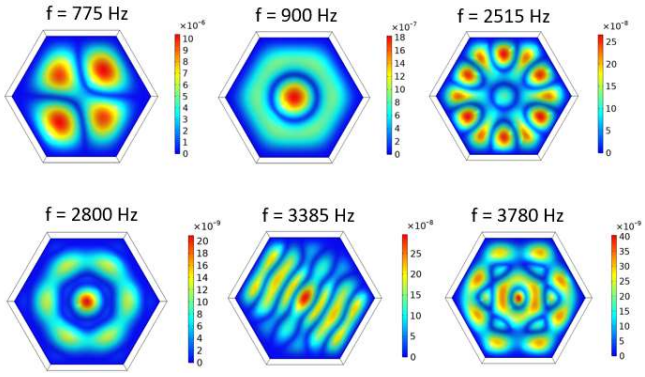

Figure 19: Displacement mode shape of the membrane for a damping loss factor of zero.

4 Honeycomb structure with multiple embedded membranes

In this section, numerical studies are carried out on the honeycomb structure with multiple embedded membrane layers.

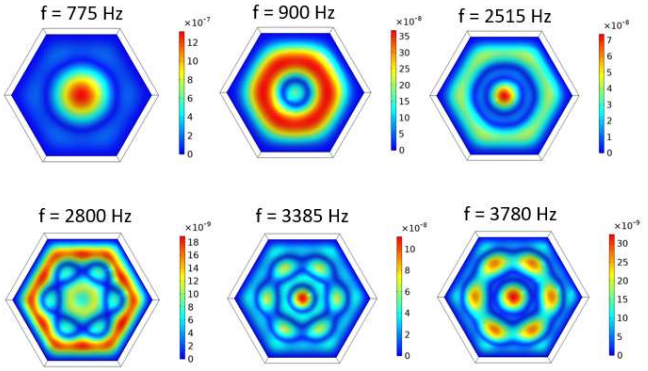

Figure 20: Displacement mode shape of the membrane for a damping loss factor of 0.2.

4.1 Honeycomb structure with two embedded membranes

Figure 21 shows a honeycomb cell with two integrated membrane layers. D represents the thickness of the air gap between the two membranes. Fixed boundary conditions are considered for each membrane with the same thickness t. The geometry is shown in Fig. 21(a) where the incident and transmission fluid have the same length. The mesh is illustrated in Fig. 21(b). Each membrane is characterized as a linear isotropic elastic material using the solid mechanics module of COMSOL and the material properties of each membrane are identical to membrane 2 of Table 1 with zero damping loss factor. An incident pressure of 1 Pa is applied on the inlet plan and the transmission loss is calculated using Eq. (1).

In Fig. 22, the influence of the thickness t of each membrane on the transmission loss is illustrated. The thickness of the air gap D is set to 10 mm and the cell size R is 5 mm.

With a thickness of 0.25 mm, the TL in Fig. 22 presents a peak at 2000 Hz with a value of 114 dB and drops to zero at the frequencies around 610 Hz, 1425 Hz, 2325 Hz and 2530 Hz. For a thickness of 0.5 mm, the TL presents a drop in the frequency range 1000-1600 Hz while outside this band, the TL is greater than 20 dB for f<1000 Hz and f>1600 Hz. With a thickness of 1 mm, the TL is greater than 30 dB for f<2000 Hz and increases when the frequency decreases.

Figure 23 shows the influence of the air gap thickness D on the transmission loss where the honeycomb cell size is set to 5 mm. Each membrane has a thickness of 0.5 mm. The TL in Fig. 23 for each value of D has two frequencies where the TL is zero. The first frequency drop of the TL around 1180 Hz is the same for all values of D. For air gap thicknesses of 3 mm, 5 mm, 10 mm, 15 mm and 20 mm, the second frequency drop is observed at 2150 Hz, 1855 Hz, 1570 Hz, 1440 Hz and 1375 Hz respectively. As D increases, the second frequency drop decreases. For D=20 mm, the frequency band where the TL drops is reduced and outside this frequency band, the TL is higher than the others. By increasing the thickness of the air gap, the TL in Fig. 23 is improved.

Figure 24 shows the impact of the cell size R on the transmission loss of the honeycomb structure with two integrated membranes layers. The thickness of each membrane is 0.5 mm with an air gap thickness D of 10 mm.

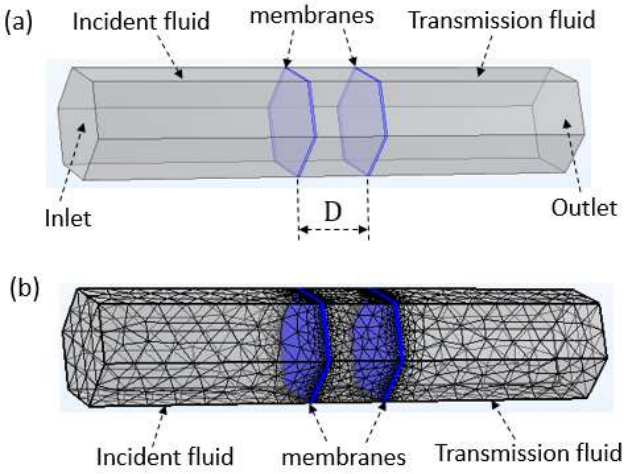

Figure 21: Honeycomb structure with two embedded membrane layers: (a) geometry (b) mesh.

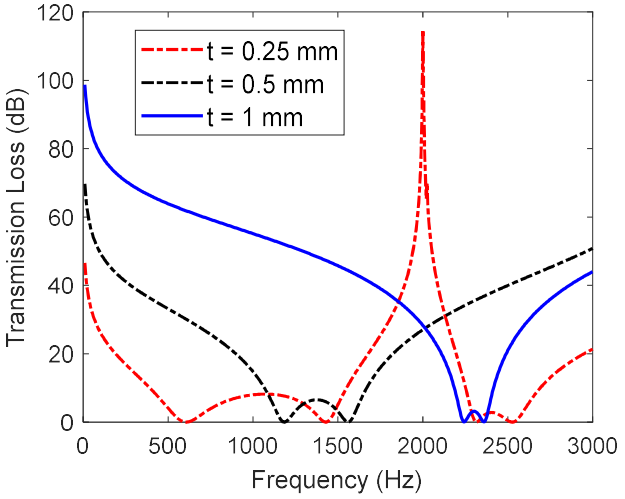

Figure 22: Effect of the membranes thickness on the transmission loss of honeycomb cell with two embedded membrane layers.

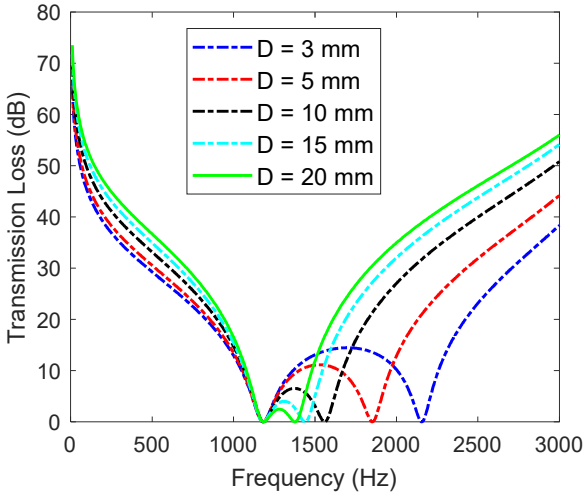

Figure 23: Effect of the air gap thickness on the transmission loss.

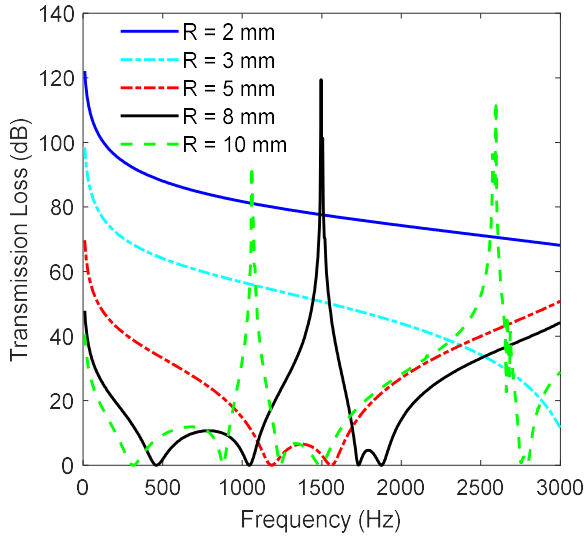

Figure 24: Effect of cell size on the transmission loss of honeycomb cell with two embedded membrane layers.

For cell dimensions of 2 mm and 3 mm, the TL in Fig. 24 exhibits a wide attenuation frequency band. For R = 2 mm, the TL is greater than 68 dB over the entire frequency range and with R=3 mm, the TL is greater than 43 dB for f<2000 Hz. With a dimension R of 5 mm, the TL presents a drop in the frequency range 1120-1640 Hz. When R is equal to 8 mm, there is a resonant frequency of 1495 Hz where the TL value reaches 119.5 dB and for R=10 mm, one observes two resonance frequencies at 1060 Hz and 2595 Hz where the TL peak values reach 92 dB and 113 dB respectively. Thus, by reducing the dimension of the honeycomb cell size, the TL increases over a wide frequency range.

4.2 Honeycomb structure with three embedded membranes

A honeycomb structure with three embedded membrane layers is shown in Fig. 25. The thickness of each membrane is set to 0.5 mm with fixed boundary conditions. The thickness of the air gap between the membranes is denoted by D_1 and D_2 and the material properties of membrane 2 in Table 1 are used for the three membranes with negligible (zero) loss factor.

The effect of the cell size R on the TL of honeycomb structure with three embedded membrane layers is shown in Fig. 26. The thickness of each air gap is set to 5 mm. For a cell dimension R of 3 mm, it is observed that the TL in Fig. 26 exhibits a wide attenuation frequency band. Three anti-resonance frequencies at 1190 Hz, 1570 Hz and 2090 Hz where the TL is zero appear for R=5 mm while there is a resonance TL peak at 1515 Hz for R=8 mm. For R=10 mm, the TL presents two resonant frequencies at 975 Hz and 2275 Hz where the TL peak values are 93 dB and 122 dB respectively. The TL frequency band is improved by reducing the cell size.

Figure 27 shows the TL for different air gap thicknesses by setting the honeycomb cell size to 5 mm.
The TL in Fig. 27 increases for f<1175 Hz when the air gap thickness increases. The three anti-resonance frequencies decrease respectively with the increase of D_1 and D_2 and the

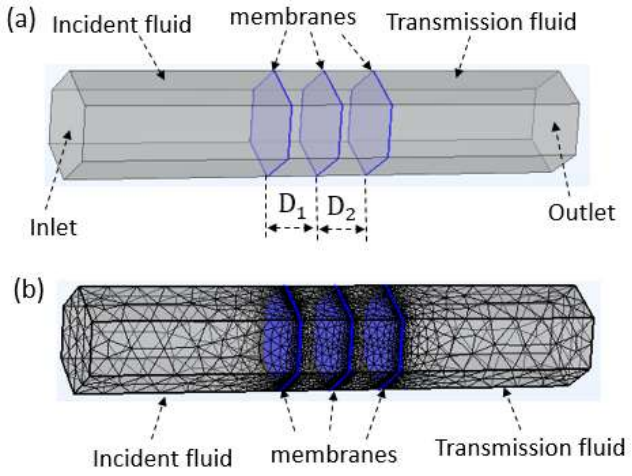

Figure 25: Honeycomb structure with three embedded membrane layers: (a) geometry (c) mesh.

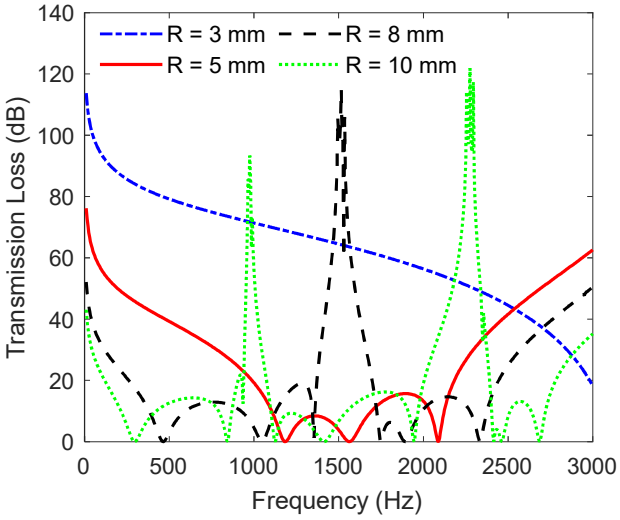

Figure 26: Effect of the cell size on the transmission loss of honeycomb cell with three embedded membrane layers.

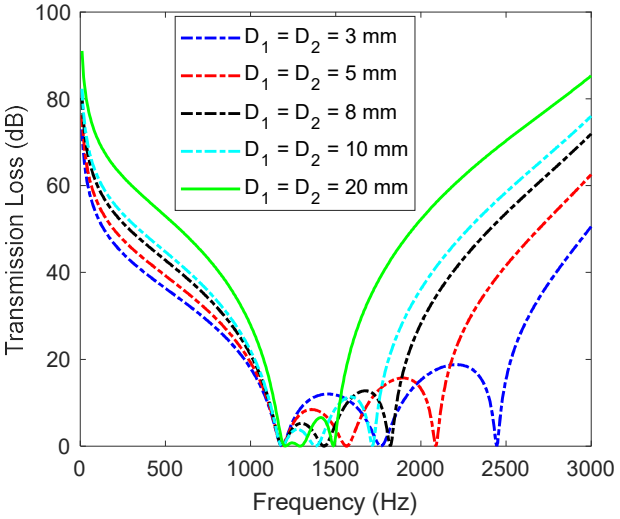

Figure 27: Effect of the air gap thickness on the transmission loss of honeycomb cell with three embedded membrane layers.

TL frequency drop band decreases.

Figure 28 illustrates the impact of the number of membrane layers within the honeycomb structure where the cell size is set to 5 mm. Membrane 2 of Table 1 with fixed boundary conditions is used with a thickness of 1 mm. For the two-membrane layer case, the thickness of the air gap D is set to 10 mm and for the three-membrane layer case; the thickness of each air gap D_1 and D_2 is set to 5 mm.

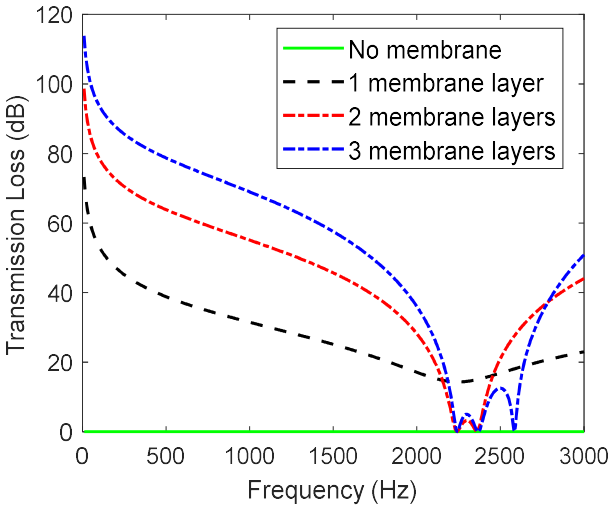

Figure 28: Effect of the number of membrane layers on the transmission loss.

The TL of the honeycomb structure alone without membrane in Fig. 28 is zero over the entire frequency range. When the number of membrane layers within the honeycomb structure increases, the TL increases for frequencies lower than 2000 Hz.

The honeycomb membrane-type acoustic metamaterial that is studied in this paper can provide engineering solutions in applications where the reduction of low frequency noise with a minimum added weight while offering structural stiffness is required. This type of metamaterial can be useful in many noise control engineering applications such as aerospace, manufacturing and process industries, and land transportations.

5 Conclusion

A honeycomb membrane-type acoustic metamaterial made of a honeycomb structure with embedded membrane layers was studied using the finite element method. The transmission loss of the metamaterial showed significant improvement especially at low frequency while the TL of the honeycomb core alone is zero over the entire frequency range. It is observed that the TL increases over a large frequency band as the honeycomb cell size is reduced and the displacement magnitude of the membrane decreases. The impact of the membrane thickness on the TL and displacement magnitude and mode shape at different frequencies were demonstrated. The TL and displacement magnitude show multiple resonant peaks as the thickness of the membrane decreases. The influence of the membrane damping loss factor was investigated. Honeycomb structures with two and three embedded membrane layers were studied numerically and the effects of the number of membrane layers and of the thickness of the air gap between membranes on the TL were presented. The TL increases over a large frequency band when the number of membrane layers within the honeycomb structure increases. The investigated metamaterial can help in low frequency noise attenuation in many engineering applications including aerospace, land transportation, and various industries.

Acknowledgments

The authors would like to acknowledge the National Research Council Integrated Aerial Mobility Program for the financial support.

References

[1] Y. Li, Y. Zhang, and S. Xie. A lightweight multilayer honeycomb membrane-type acoustic metamaterial. Applied Acoustics, 168: 107427, 2020.

[2] N. Sui, X. Yan, T.-Y. Huang, J. Xu, F.-G. Yuan, and Y. Jing. A lightweight yet sound-proof honeycomb acoustic metamaterial. Appl. Phys. Lett. 106: 171905, 2015.

[3] K. Lu, J.H. Wu, D. Guan, N. Gao, and L. Jing. A lightweight low-frequency sound insulation membrane-type acoustic metamaterial. AIP Advances 6, 025116, 2016.

[4] H. Nguyen, Q. Wu, J. Chen, Y. Yu, H. Chen, S. Tracy, and G. Huang. A broadband acoustic panel based on double-layer membrane-type metamaterials. Appl. Phys. Lett. 118: 184101, 2021.

[5] Z. Yang, J. Mei, M. Yang, N.H. Chan, and P. Sheng. Membrane-type acoustic metamaterial with negative dynamic mass. Phys. Rev. Lett., 101:1–4, 2008.

[6] S. Li, D. Mao, S. Huang, and X. Wang. Enhanced transmission loss in acoustic materials with micro-membranes. Applied Acoustics, 130: 92–98, 2018.

[7] S. Qiu, S. Li, X. Wang, and D. Mao. Enhanced transmission loss through lattice-supported micro-membranes. Applied Acoustics, 153, 127–131, 2019.

[8] Z. Laly, C. Mechefske, S. Ghinet, B. Ashrafi, and C.T. Kone. Numerically analysis of honeycomb structure with embedded membrane for transmission loss improvement. Canadian Acoustics Proceedings, 50(3), 22-23, 2022.

[9] Nansha Gao, Hong Hou, and Jiu Hui Wu. A composite and deformable honeycomb acoustic metamaterial. International Journal of Modern Physics B 32(20), 1850204, 2018.

[10] Haoming Hu, Shuai Zhu, and Hongyu Cui. Sound insulation performance of Mis-haped mass membrane-honeycomb structure acoustic metamaterials. Proc. SPIE 12164, International Conference on Optoelectronic Materials and Devices, ICOMD 2021, Guangzhou, China.

[11] Fuyin Ma, Meng Huang, and Jiu Hui Wu. Ultrathin lightweight plate-type acoustic metamaterials with positive lumped coupling resonant. JOURNAL OF APPLIED PHYSICS 121, 015102, 2017.

[12] Polina Marinova, Stephan Lippert, and Otto von Estorff. On the numerical investigation of sound transmission through double-walled structures with membrane-type acoustic metamaterials. J. Acoust. Soc. Am. 142 (4), 2400–2406, 2017.

[13] Guojian Zhou, Jiu Hui Wu, Kuan Lu, Xiujie Tian, Xiao Liang, Wei Huang and Keda Zhu. An approach to broaden the low-fre-

quency bandwidth of sound insulation by regulating dynamic effective parameters of acoustic metamaterials. J. Phys. D: Appl. Phys. 52 215102, 2019.

[14] Juan Mo, Zongren Peng and Xu Wang. Achieving Enhanced Sound Insulation through Micromembranes-Type Acoustic Metamaterials. Appl. Sci. 12, 1950, 2022.

[15] F. Langfeldt, W. Gleine and O. von Estorff. An efficient analytical model for baffled, multi-celled membrane-type acoustic metamaterial panels. Journal of Sound and Vibration 417, 359–375, 2018.

[16] Z. Laly, C. Mechefske, S. Ghinet, B. Ashrafi, and C.T. Kone. Finite element design of acoustic metamaterial based on parallel Helmholtz resonators with embedded membranes. Canadian Acoustics Proceedings, 50(3), 20-21, 2022.

[17] Z. Laly, C. Mechefske, S. Ghinet, and C.T. Kone. Numerical modelling of acoustic metamaterial made of periodic Helmholtz resonator containing a damping material in the cavity. In Proceedings of 2022 Inter-national Congress on Noise Control Engineering, INTER-NOISE 2022, 21-24 August 2022, Glasgow, UK.

[18] Z. Laly, C. Mechefske, S. Ghinet, C.T. Kone and N. Atalla. Modelling of acoustic metamaterial sound insulator using a transfer matrix method for aircraft cabin applications. In Proceedings of 2022 Inter-national Congress on Noise Control Engineering, INTER-NOISE 2022, 21-24 August 2022, Glasgow, UK.

[19] Z. Laly, C. Mechefske, S. Ghinet, and C.T. Kone. Numerical design of acoustic metamaterial based on parallel Helmholtz resonators for multi-tonal noise control. In Proceedings of 2022 International Congress on Noise Control Engineering, INTERNOISE 2022, 21-24 August 2022, Glasgow, UK.